UDC 699 . 841 : 691 . 714 : 620 . 178 . 3

Fatigue Properties of Practical-Scale Unbonded Braces

Hiroshi NAKAMURA*1
Yasushi MAEDA*1
Takao SASAKI*2
Akira WADA*4
Toru TAKEUCHI*1
Yasuhiro NAKATA*1
Mamoru IWATA*3

Abstract

Damages inflicted on beam ends of steel structure buildings during the big earthquake in the Hanshin-Awaji area in January, 1995 aroused interest in a damping method (damage controlling method) whereby the main structure portion is kept at the elastic region by use of hysteresis dampers behaving plastically from low force input levels. This paper describes studies on performance limits of unbonded braces as hysteresis dampers based on tests on fatigue properties of practical-scale unbonded braces. Tests showed that the number of cycles for causing material failure was approximately 200 when the equivalent story drift angle was 1/100, the result of which was proof enough that the braces have good fatigue properties in consideration of accumulated plastic deformation factor. This paper also shows that the same fatigue properties can be obtained when different steel grades (JIS SN400B, and Nippon Steel's specifications LYP100 and LYP235) are used for the cores of the braces. From comparative studies with material fatigue tests and model tests of the brace core, the fatigue properties of the practical-scale unbonded braces were found to decrease due to factors such as local buckling of the brace core. A formula is proposed herein for expressing a fatigue curve in consideration of strain concentration and it is demonstrated that the proposed formula can estimate fatigue life of the braces.

1. Introduction

Through the conventional earthquake resistant design of building, earthquake resistance was secured by absorption of seismic energy through plastic deformation of columns and beams of the structure. At the Hansin-Awaji Earthquake in 1995, however, there were many cases where damages such as residual plastic deformations of main structures, deformed weld joints at beam ends and so forth were inflicted on buildings, even where there was no human casualty. This was regarded as a serious problem since those damages made repair of the buildings difficult resulting in substantial losses of property values. For this reason, a new damage control design (damping design) has become popular lately[1-4] whereby the main structure is kept

*1 Building Construction Division
*2 Sagamihara Research & Development Division
*3 Professor of Kanagawa University
*4 Professor of Tokyo Institute of Technology

in the elastic region by concentrating the seismic energy to hysteresis dampers or something similar strategically arranged in the structure and made to behave plastically from low force input levels. This method increases the possibility of reusing the main structure of the building simply by replacing the dampers after a disaster.

While the main structure survives, the dampers repeatedly undergo far severer plastic strains than the other structural members do. Accordingly, together with maximum plastic deformation capacity, low cycle fatigue properties in the plastic region of the hysteresis dampers are one of the most important indicators to judge their service life. A variety of research results have been reported in relation to these aspects either from the viewpoint of the steel material or the structural member[5-10].

With regards to unbonded braces developed as earthquake-resistant structural members, the required properties for making them usable as the hysteresis dampers have so far been examined. As the final stage following fatigue tests of the steel materials[11] and those of the unbonded brace cores in consideration of stress concentration on the welds at rib ends[12], the fatigue properties of the unbonded braces as structural members, as described herein, in consideration of strain concentration due to local buckling of the core inside a restriction casing were studied in experiments. It was expected that these studies would clarify the performance limit of the unbonded braces when used as hysteresis dampers.

It is intended in this paper to clarify hysteresis stability and fatigue failure characteristics of the braces by experimentally confirming, through fatigue tests of practical-scale unbonded braces, their capacity of accumulated plastic deformation, the number of loading cycles to cause material failure and failure conditions. Furthermore, discussed herein are the interrelations between the results of the above final studies and those of the previous studies reported in reference papers 11) and 12).

2. Outline of Tests

2.1 Steel materials

Three steel grades were selected for the damper cores as having excellent properties for the hysteresis dampers, namely, a rolled steel for building structure (JIS SN400B) and two low yield point steels (Nippon Steel's specifications BT-LYP100 and BT-LYP235, hereinafter being called LYP100 and LYP235, respectively). The mechanical properties and chemical compositions of these steels are shown in **Tables 1 and 2**.

Table 1 Mechanical properties of material

Series	Steel grade	Thickness (mm)	Yield point (N/mm²)	Tensile strength (N/mm²)	Elongation (%)
TP-1, 2	LYP100	25	95	249	84
TP-3	SN400B	25	259	426	35
TP-4	LYP235	16	239	334	60
TP-5	LYP235	28	222	324	69

Table 2 Chemical composition of material

Series	Steel grade	Thickness (mm)	C (%)	Si (%)	Mn (%)	P (%)	S (%)
TP-1, 2	LYP100	25	0.001	0.01	0.07	0.009	0.004
TP-3	SN400B	25	0.16	0.17	0.67	0.020	0.007
TP-4	LYP235	16	0.01	0.01	0.49	0.023	0.010
TP-5	LYP235	28	0.01	0.01	0.49	0.023	0.010

2.2 Shape of test specimens

Shape and size of test specimens were roughly the same as the real unbonded braces as seen in **Fig. 1** in detail. LYP100 was used for the cores of TP-1 and 2, and SN400B for those of TP-3. TP-4 and 5, which had cores made of LYP235, were modified shape unbonded braces having a shorter portion for plastic deformation (roughly 1/3 of the others) in order to increase apparent axial stiffness.

2.3 Test parameters

Data of the test specimens are given in **Table 3**. Here, the word "core" indicates the portion of the unbonded brace where it behaves plastically, "strain (ε)" the strain of the core thus defined, and "strain amplitude ($\Delta\varepsilon_t$)" the sum of the compression strain and the tension strain of the core as shown in **Fig. 2**. Axial strain of the portion of the test specimen excluding the joints at both the ends is referred to as "mean strain (ε_a)" and the sum of the compression strain and the tension strain of said portion "mean strain amplitude ($\Delta\varepsilon_a$)." Consequently, whereas the strain amplitude ($\Delta\varepsilon_t$) and the mean strain amplitude ($\Delta\varepsilon_a$) are equal in TP-1 to 3 in which the core length and the mean strain portion length are the same, the former ($\Delta\varepsilon_t$) is larger than the latter ($\Delta\varepsilon_a$) in TP-4 and 5 in which the core length is smaller as shown in Table 3. The value of the controlled displacement in Table 3 for each test specimen was set in consideration of the elastic deformation of the joints at both the ends so that a predetermined amount of strain amplitude ($\Delta\varepsilon_t$) would be imposed on the core. The

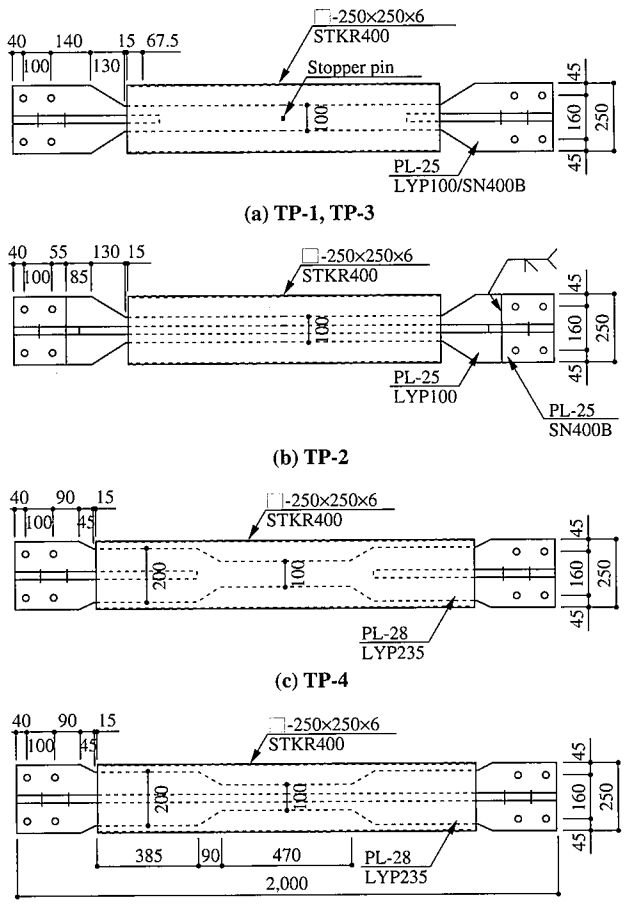

Fig. 1 Detail drawings of test specimens

Table 3 Test specimen data

Series	Test specimen name	Steel grade	Core section shape	Core thickness (mm)	Core width (mm)	Core section area (cm^2)	Member length (mm)	Core length (mm)	Mean strain portion length (mm)	Concentration ratio α	Yield axial force (kN)	Strain amplitude (%)	Strain velocity (%/s)	Controlled displacement (mm)	Equivalent story drift angle
TP-1	100–150	LYP100	–	25	100	25	2,000	960	960	1.0	320	1.5	0.1	±7.3	1/100
	100–040	LYP100	–	25	100	25	2,000	960	960	1.0	320	0.4	0.1	±2.0	1/375
	100–016	LYP100	–	25	100	25	2,000	960	960	1.0	320	0.16	0.1	±0.8	1/938
TP-2	100+150	LYP100	+	25	100	44	2,000	1,180	1,180	1.0	563	1.5	0.1	±8.9	1/100
TP-3	400-200	SN400B	–	25	100	25	2,000	960	960	1.0	665	2.0	0.1	±9.8	1/75
	400–150	SN400B	–	25	100	25	2,000	960	960	1.0	665	1.5	0.1	±7.4	1/100
	400–040	SN400B	–	25	100	25	2,000	960	960	1.0	665	0.4	0.1	±2.0	1/375
TP-4	235+150	LYP235	+	16	100	29	2,000	470	1,450	3.1	693	4.3(1.5)	0.29(0.1)	±10.9	1/100
	235+016	LYP235	+	16	100	29	2,000	470	1,450	3.1	693	0.26(0.16)	0.16(0.1)	±1.2	1/938
TP-5	235–150	LYP235	–	28	100	28	2,000	470	1,450	3.1	669	4.5(1.5)	0.3(0.1)	±10.9	1/100
	235–016	LYP235	–	28	100	28	2,000	470	1,450	3.1	669	0.36(0.16)	0.23(0.1)	±1.2	1/938

Note: The values in parentheses of TP-4 and 5 are mean strain amplitude and mean strain velocity. The values of equivalent story drift angle correspond to a core length of 1/1.5 of the distance between column/beam joints and a brace angle of 45°.

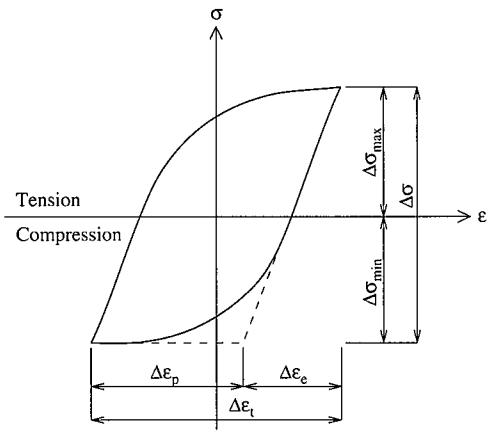

Fig. 2 Symbol definitions

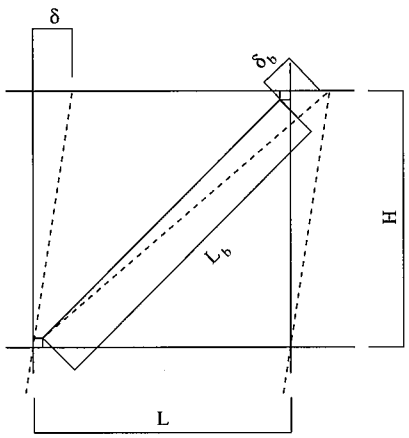

Fig. 3 Frame deformation

concentration ratio (α) is the ratio of the mean strain portion length to the core length.

The unbonded brace test specimens were given different steel materials and core section shapes for the purpose of observing their fatigue properties under different values of the strain amplitude ($\Delta\varepsilon_t$). The maximum strain amplitude in the present tests corresponds to an equivalent building story drift angle (δ/H in **Fig. 3**) of approximately 1/75 as shown in Table 3. It should be noted that the strain amplitude of the test specimen cores was correlated to the equivalent story drift angle on an assumption that there would be a strain concentration of 1.5 times that in the distance between the joints, in consideration of the influence of the joints at both the ends.

2.4 Test method

Alternate loads were imposed on the test specimens in the axial direction, by a 2,000KN actuator using a 1,400KN reaction frame, under a displacement control such that a predetermined amount of axial displacement (axial strain) took place. The test specimen was firmly fixed to the reaction frame at the lower end, and horizontal displacement of its upper end was restricted. **Photo 1** shows a scene of the loading test.

2.5 Loading program

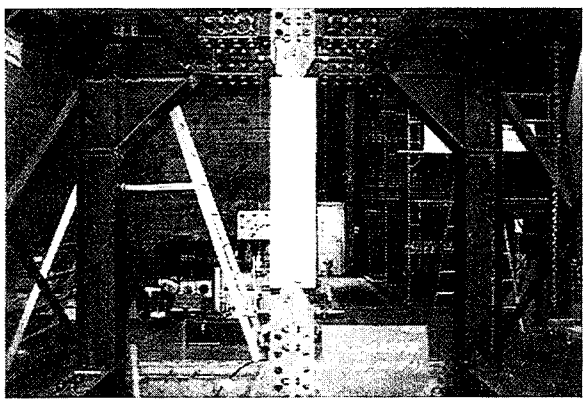

Photo 1 Loading

Fig. 4 schematically shows a loading cycle. An axial force roughly 50% of the yield axial force of the test specimen was imposed in the first loop as a break-in of the test specimen and the jigs. Then, the amount of the controlled displacement specified in Table 3 was im-

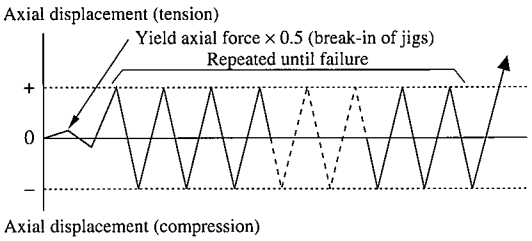

Fig. 4 Loading cycle

posed cyclically, under a displacement control to make the strain velocity constant, until the core failed. In the initial stage of the loading operation, the amount of axial displacement was gradually increased to attain the predetermined amount of controlled displacement. For this reason, counting of the number of the cycles began with the cycle where the predetermined displacement amount was attained.

3. Test Results and Discussion

3.1 Change of axial force

Fig. 5 (a) to (d) show the relationship between the stress range ($\Delta\sigma$) and the number of the loading cycles (N) of each of the test specimen series TP-1 to 5. Here we see no extreme stress increase and fluctuation during the course of the loading cycles in any of the test results. The reason why all the test specimens showed strain-hardened stress from the first cycle is that several preliminary cycles were imposed on the test specimen with gradually increasing loads until the predetermined amount of controlled displacement was attained, and the preliminary cycles were not counted.

3.2 Change of hysteresis characteristics

Fig. 6 shows the stress (σ)-strain (ε) relationship of the test specimen 100-150 under the maximum axial force and at the number of the cycle (N_f-th cycle) when material failure took place (the number being hereinafter referred to as the "failure cycle number"). Here we see that the stress-strain loops in both the situations are nearly identical. The same tendency was seen also with the other test specimens. This is because the failure cycle number was defined as the cycle where the test specimen could not withstand the load (when the loading cycle loop was so deformed that it did not form a closed loop) any longer. During the course of the present tests, there were only three cases where the failure cycle number (N_f) was determined by 75% of the maximum load as we reported previously[2]. (See **Table 4**.)

3.3 Number of cycles to cause material failure

The failure cycle number (N_f) is shown in Table 4 for each test specimen. Here N_f is defined as the number of the loading cycle (N_f-th cycle) where the axial force falls to 75% of the maximum axial force or the same where the hysteresis characteristics become unstable due to a failure, whichever is the smaller.

As stated in 3.2 above, we see in Table 4 that only three test specimens failed at 75% of maximum axial force and all the rest failed when they could not withstand the imposed load any more. We can also see that, under roughly the same strain amplitudes, the – section shape cores showed better fatigue performance than the + section shape cores. In terms of the failure cycle number, the braces withstood roughly 200 cycles (30 cycles in the case of the modified shape specimens) of an equivalent story drift angle of 1/100, demonstrating sufficiently high accumulated deformation performance.

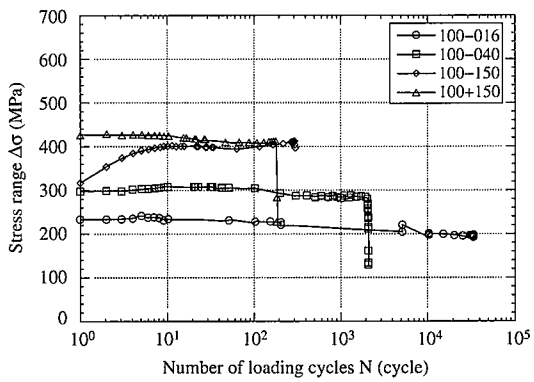

(a) TP-1, TP-2

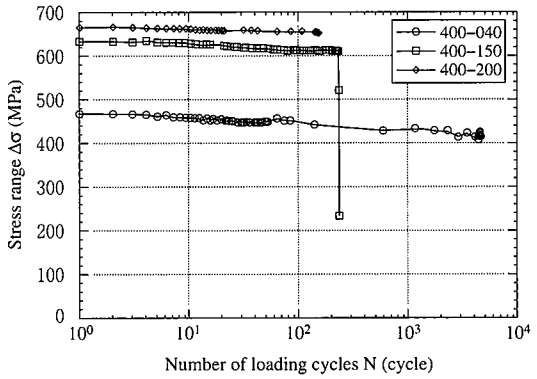

(b) TP-3

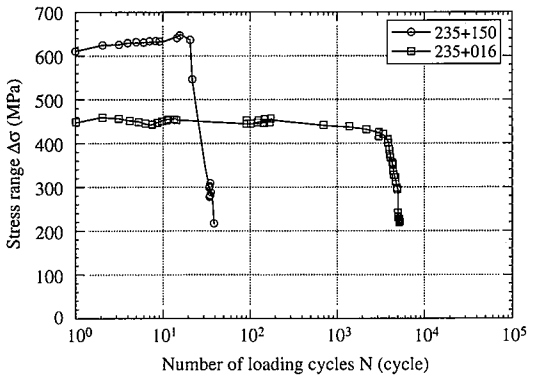

(c) TP-4

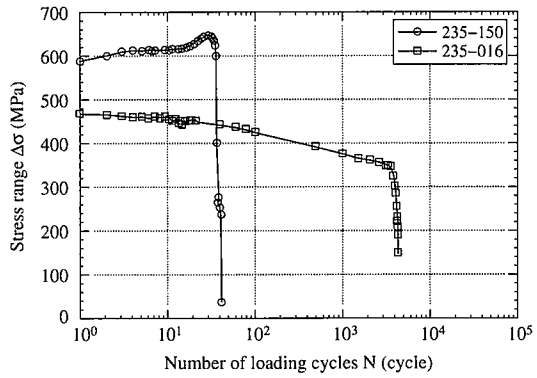

(d) TP-5

Fig. 5 Relationship between stress range ($\Delta\sigma$) and number of loading cycles (N)

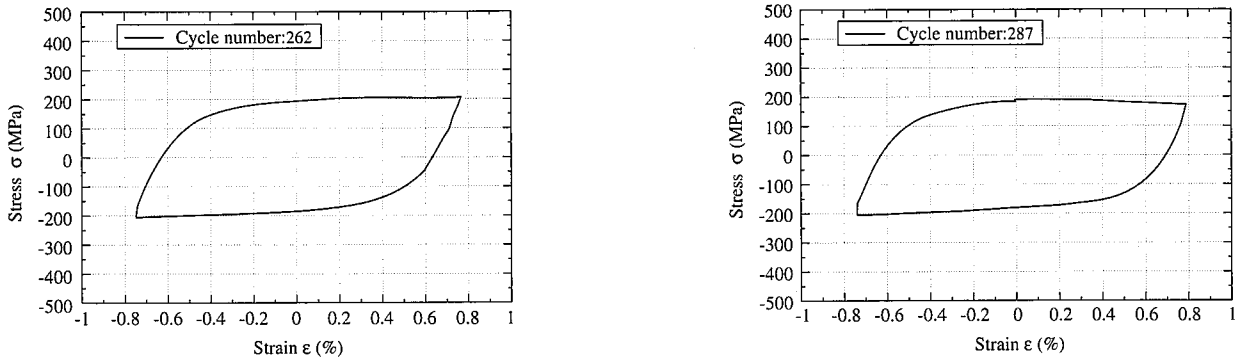

(a) Maximum axial force (b) Cycle when material failed

Fig. 6 Stress (σ) – strain (ε) relationship (100–150)

Table 4 Number of cycles to cause material failure

Series	Test specimen name	Steel grade	Core section shape	Concentration ratio α	Strain amplitude $\Delta\varepsilon_t$ (%)	Equivalent story drift angle	Number of cycles to cause material failure N_f (cycle)	Failure position	Accumulated plastic deformation factor η_f
TP-1	100–150	LYP100	–	1.0	1.5	1/100	287 (Loop)	Stopper	17,504
	100–040	LYP100	–	1.0	0.4	1/375	2,041 (75% of maximum axial force)	Rib end	27,208
	100–016	LYP100	–	1.0	0.16	1/938	33,451 (Loop)	Middle	98,085
TP-2	100+150	LYP100	+	1.0	1.5	1/100	176 (Loop)	Middle	10,734
TP-3	400–200	SN400B	–	1.0	2.0	1/75	140 (Loop)	Stopper	3,890
	400–150	SN400B	–	1.0	1.5	1/100	211 (Loop)	Stopper	4,186
	400–040	SN400B	–	1.0	0.4	1/375	4,050 (Loop)	Middle	9,545
TP-4	235+150	LYP235	+	3.1	4.3 (1.5)	1/100	18 (Loop)	Middle	1,261 (393)
	235+016	LYP235	+	3.1	0.26 (0.16)	1/938	4,150 (75% of maximum axial force)	Rib end	1,982 (0)
TP-5	235–150	LYP235	–	3.1	4.5 (1.5)	1/100	33 (Loop)	Middle	2,621 (786)
	235–016	LYP235	–	3.1	0.36 (0.16)	1/938	2,520 (75% of maximum axial force)	Rib end	6,740 (0)

Note: The values in parentheses of TP-4 and 5 are mean strain amplitude and mean strain velocity. The values of equivalent story drift angle correspond to a core length of 1/1.5 of the distance between column/beam joints and a brace angle of 45°.

From the fact that TP-1 to 3 showed a fatigue performance to withstand more than 10^4 cycles of an equivalent story drift angle of 1/1,000, there is a possibility that unbonded braces are used also as vibration dampers against winds.

3.4 States of failures

Failure positions of the test specimens are listed in Table 4, the position definitions being given in **Fig. 7**. The cores of the test specimens having comparatively large strain amplitudes (100–150, 400–200 and 400–150) failures near the stopper pin at the center, presumably due to stress concentration at the welded joint of the stopper pin. In contrast, the cores of the other test specimens of smaller strain amplitudes broke at the end of the reinforcing ribs at an end of the brace or between the stopper pin and the rib end. It was also observed that the test specimens having comparatively large strain amplitudes showed very coarse fracture grain, indicating rapid propagation of the failure, typical of the surfaces of low cycle fatigue failure. (See **Photo 2**.) On the other hand, in the cases where the strain amplitude was smaller, the grain size at the failure surface was fine, indicating that the failure propagated slowly. (See **Photo 3**.)

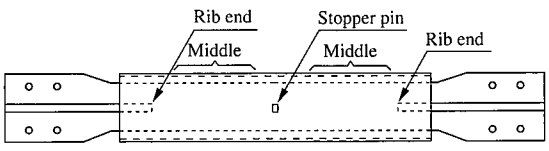

Fig. 7 Failure positions

3.5 Accumulated plastic deformation factor

Also listed in Table 4 is accumulated plastic deformation factor (η_f), which is the ratio of accumulated plastic strain to yield strain (yield point/elastic modulus).

From the accumulated plastic deformation factor (η_f) in the table, it is clear that all the test specimens have good deformation properties. The η_f values for the mean strain amplitude of the modified shape braces, TP-4 and 5, are 0. This is because the axial deformation was too small for the standard type braces (such as TP-1 to 3) to yield, and this result shows that the modified shape braces functioned as hysteresis dampers even under such a condition.

3.6 Comparison with results of material tests and core model tests

Fig. 8 (a) and (b) compare the relationship between the failure cycle number (N_f) and the strain amplitude ($\Delta\varepsilon_t$) obtained in the present tests (TP-1 to 3) with the same obtained in the material tests and the core model tests[12], by steel grade (LYP100 and SN400B). The values of the failure cycle number (N_f) in the core model tests

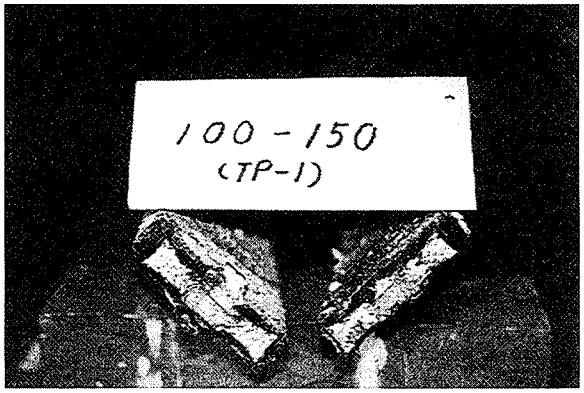

Photo 2 Failure of 100–150

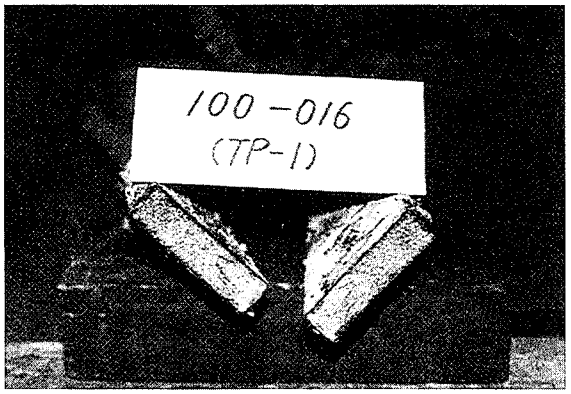

Photo 3 Failure of 100–016

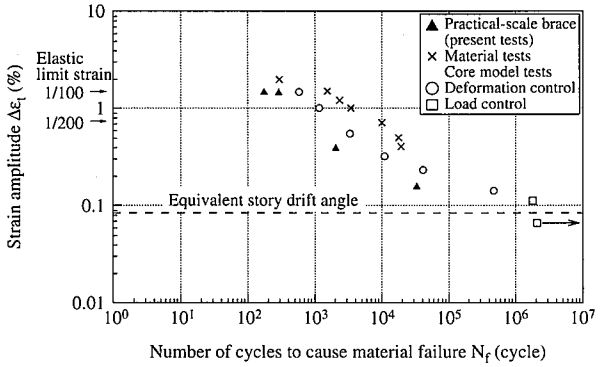

(a) LYP100

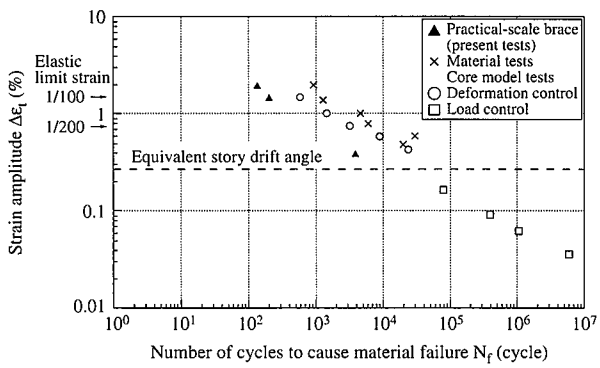

(b) SN400B

Fig. 8 Relationship between number of cycles to material failure (N_f) and strain amplitude ($\Delta\varepsilon_t$)

were 1/2 to 1/5 of those in the material tests, and those in the practical-scale tests were 1/6 to 1/10, presumably because of influences of stress concentration at the ends of the reinforcing ribs or that caused by local buckling. LYP100 and SN400B showed nearly identical plastic fatigue characteristics.

3.7 Fatigue properties of practical-scale unbonded braces in consideration of strain concentration

Fig. 9 shows test results of the strain amplitude of the core ($\Delta\varepsilon_t$) and the failure cycle number (N_f) and their regression curves (α =1.0). It also shows the test results of the mean strain amplitude ($\Delta\varepsilon_a$) and the failure cycle number (N_f) of TP-4 and 5 (solid circles, α = 3.1). The following equation is derived from the regression curves taking into consideration the relationship between the mean strain amplitude ($\Delta\varepsilon_a$) and strain amplitude of the core ($\Delta\varepsilon_t$):

$$\Delta\varepsilon_a\,(\%) = (20.48/\alpha)\cdot N_f^{-0.49} \qquad (1)$$

where concentration ratio (α) is the quotient of the mean strain portion length of each test specimen divided by its core length, and its values are shown in Tables 3 and 4. Accordingly, $\Delta\varepsilon_a = \Delta\varepsilon_t$ when α = 1. It should be noted that the influence of stiffness of the portion of the mean strain portion less the core length is neglected in Equation (1). Fig. 9 also shows fatigue curves corresponding to various values of the concentration ratio (α) based on Equation (1) in dotted lines.

The results of the present tests made it clear that there was no marked difference in the fatigue life among SN400B, LYP100 and LYP235 and that roughly the same fatigue curve could be applied to all of them. It was also observed that, according to the test results of LYP235 (solid circles), its fatigue life tended to become shorter as the concentration ratio (α) increased and it could be roughly estimated by the fatigue curves expressed by Equation (1).

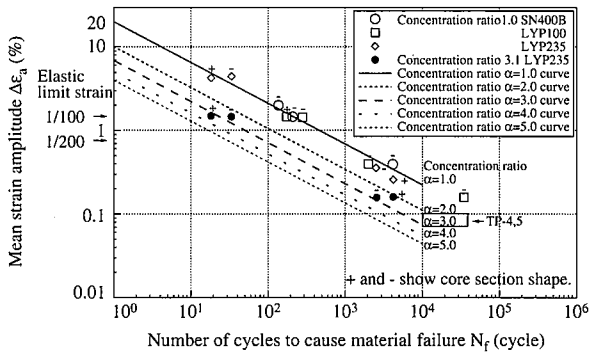

Fig. 9 Fatigue curves of unbonded braces considering strain concentration

4. Recorder of Maximum and Accumulated Deformation

In the present tests, each of 100–150 and 400–040 was tested with a maximum deformation recorder installed at its upper end to record the largest deformation inflicted on it in the past and an accumulated deformation recorder installed at the lower end to record the accumulated deformation. The recorders are shown in **Photos 4 and 5**, respectively, and the recorded results in **Table 5**. The estimated values in the table are what the recorders should have recorded if they had worked ideally. The recorded results conformed to them in the maximum compression deformation, but somewhat deviated in

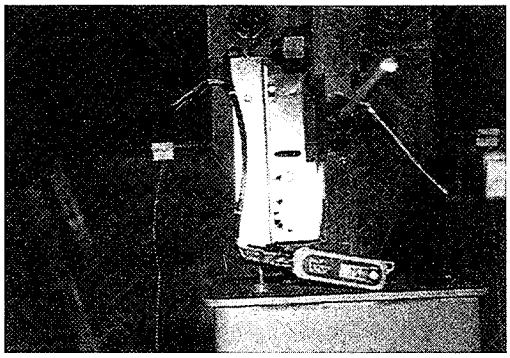

Photo 4 Maximum deformation recorder

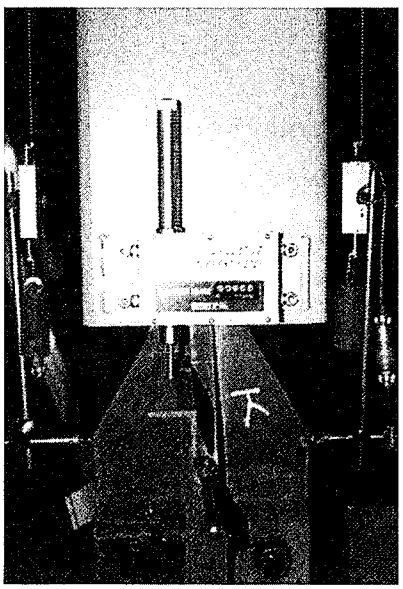

Photo 5 Accumulated deformation recorder

the maximum tensile deformation and the accumulated deformation. The deviations were caused probably by buckling restriction cases, which moved slightly downwards during the repeated loading.

5. Summary

The present tests clarified the fatigue properties of practical-scale unbonded braces and confirmed the fact that they have sufficient performance as hysteresis dampers, especially:

(1) that the unbonded braces can withstand roughly 200 cycles of loads of an axial strain of ±0.75% on the core, which strain corresponds to a equivalent story drift angle of 1/100, before material failure takes place, and

(2) that the modified shape unbonded braces, which have a strain concentration (α) three times that of the normal braces, can withstand roughly 30 cycles of loads corresponding to an equivalent story drift angle of 1/100 before material failure takes place.

Since it has been known that the energy input of one earthquake corresponds to approximately 2 hysteresis loops of the maximum axial deformation[13], it is expected:

(3) that the modified shape unbonded braces can be used as dampers through more than 15 big earthquakes causing a maximum instantaneous story drift angle of about 1/100 (maximum speed of roughly 40 - 50 kine), without requiring replacement as far as their fatigue performance is concerned, and that the normal unbonded braces can be used through roughly 100 earthquakes of the same strength.

If equipped with the unbonded braces as the hysteresis dampers, a building main structure is expected to suffer a very small residual deformation at an earthquake, and this small deformation can be removed by dismounting the unbonded braces for replacement or reuse, making it highly probable that the main structure continues its service life.

References

1) Iwata, M., Huang, Y.H., Kawai, H., Wada, A.: Study on The-Damage Tolerant Structures. Trans. Architectural Inst. Jap. (1), 82-87(Dec. 1995)
2) Hayashi, K., Unno, T., Iwata, M.: Damage-Controlled Structure to Diagonal Lattice Tube Frame Building. Trans. Architectural Inst. Jap.(6), 65-69(Oct. 1998)
3) Matsuoka, Y., Iwata, M., Kawai, H., Wada, A., Huang, Y.H.: Study of Damage-Tolerant Structure - Part 1: Seismic Responses Related with Yield Shear Level of Earthquake Resisting Elements. Summaries of Technical Papers of Annual Meeting (Hokkaido), Architectural Inst. Jap. 22072,1995-8, p. 143-144
4) Matsuoka, Y., Iwata, M., Kawai, H., Wada, A., Huang, Y.H.: Study of Damage-Tolerant Structure - Part 2: Hysteretic Damper that can Control Yield Point. Summaries of Technical Papers of Annual Meeting (Hokkaido), Architectural Inst. Jap. 22073,1995-8, p.145-146
5) Yamaguchi, T., Nakata, Y., Takeuchi, T., Ikebe, T., Nagao, T., Minami, A., Suzuki, T.: Seismic Control Devices Using Low-Yield Point Steel. Shinnittetsu-Giho. NSTR.(368), 61-67(1998)
6) Saeki, E., Sugisawa, M., Yamaguchi, T., Mochizuki, H., Wada, A.: A Study on Hysteresis and Hysteresis Energy Characteristics of Low Yield Strength Steel. J. Struct. Constr. Eng. AIJ.(473), 159-168(1995)
7) Saeki, E., Maeda, Y., Nakamura, H., Midorikawa, M., Wada, A.: Experimental Study on Practical-Scale Unbonded Braces. J. Struct. Constr. Eng. AIJ.(476), 149-158(1995)
8) Fujimoto, M., Wada, A., Saeki, E., Takeuchi, T., Watanabe, A.: Development of Unbonded Brace. The Column (quarterly). (115), 91-96(****)
9) Maeda, Y., Nakamura, H., Takeuchi, T., Nakata, Y., Iwata, M., Wada, A.: Fatigue Properties of Practical-Scale Unbonded Braces - Part 1: Test Program and Outline Results. Summaries of Technical Papers of Annual Meeting, (Chugoku), Architectural Inst. Jap. 1999-9
10) Nakamura, H., Maeda, Y., Takeuchi, T., Nakata, Y., Iwata, M., Wada, A.: Fatigue Properties of Practical-Scale Unbonded Braces - Part 2: Test Results. Summaries of Technical Papers of Annual Meeting (Chugoku), Architectural Inst. Jap. 1999-9
11) Saeki, E., Sugisawa, M., Yamaguchi, T., Mochizuki, H., Wada, A.: A Study on Low Cycle Fatigue Characteristics of Low Yield Strength Steel. J. Struc. Const. Eng.AIJ.(472), 139-147(1955)
12) Maeda, Y., Nakata, Y., Iwata, M., Wada, A.: Fatigue Properties of Axial-Yield Type Hysteresis Dampers. J. Struc. Const. Eng.AIJ.(503), 109-115(1998)
13) Harada, Y., Akiyama, H.: Seismic Design of Flexible-Stiff Mixed Frame with Energy Concentration. J. Struc. Const. Eng.AIJ.(472), 57-66(1995)

Table 5 Recording of maximum and accumulated deformation

Series	Test specimen name	Controlled displacement (mm)	Estimated values (mm)		Recording of maximum deformation recorder		Recording of accumulated deformation recorder	
			Maximum deformation	Accumulated deformation	Tension (mm)	Compression (mm)	Counter reading	Deformation (mm)
TP-1	100-150	±7.3	±3.0	2,161	15	3	999	1,998
TP-3	400-040	±2.0	±1.0	8,086	3	1	3,160	6,320